Chimera states on the route from coherence to rotating waves

Patrycja Jaros,[1] Yuri Maistrenko,[1,2] and Tomasz Kapitaniak[1]

[1]*Division of Dynamics, Technical University of Lodz, Stefanowskiego 1/15, 90-924 Lodz, Poland*

[2]*Institute of Mathematics and Centre for Medical and Biotechnical Research, National Academy of Sciences of Ukraine, Tereshchenkivska St. 3, 01030, Kyiv, Ukraine*

(Received 14 August 2014; revised manuscript received 15 December 2014; published 10 February 2015)

We report different types of chimera states in the Kuramoto model with inertia. They arise on the route from coherence, via so-called solitary states, to the rotating waves. We identify the wide region in parameter space, in which a different type of chimera state, i.e., the imperfect chimera state, which is characterized by a certain number of oscillators that have escaped from the synchronized chimera's cluster, appears. We describe a mechanism for the creation of chimera states via the appearance of the solitary states. Our findings reveal that imperfect chimera states represent characteristic spatiotemporal patterns at the transition from coherence to incoherence.

DOI: 10.1103/PhysRevE.91.022907 PACS number(s): 05.45.Ra, 05.45.Xt, 89.75.−k

I. INTRODUCTION

Chimera states are the spatiotemporal patterns in which synchronized and phase locked oscillators coexist with desynchronized and incoherent ones [1–25]. Dynamically chimeras represent a sort of spatially extended symmetry breaking which develops in the networks of identical oscillators without any evidence of asymmetry or external perturbation. This hybrid behavior obeys a substantial reserve of robustness surviving at different kinds of perturbations [5]. In the last decade, chimera states have been observed not only in analytical studies and numerical simulations of various networks [1–20], but also in the experimental optical [21,22], chemical [14], electronic [23], and mechanical [24,25] systems as well. Recently, in [26], the role of so-called solitary states for the desynchronization in networks with attractive and repulsive interactions has been studied. It was shown that if attractive and repulsive groups act in the antiphase or close to that, a solitary state emerges with a single repulsive oscillator which splits up from the others fully synchronized. With further increase of the repulsing strength, the synchronized cluster becomes fuzzy and the dynamics is given by a variety of stationary states with zero common forcing. The solitary states represent the natural link between coherence and incoherence, but their role in the creation of chimera states has not been investigated.

In this paper, we consider the Kuramoto model with inertia, i.e., the network of nonlocally coupled pendulumlike nodes. We analyze spatiotemporal patterns characteristic of the transition from a coherent synchronized state to a rotating wave. We identify a mechanism for the creation of chimera states via the appearance of the solitary states. Investigating the transition between complete synchronization and the chimera state, we have observed regions in parameter space, where one or a few oscillators escaped from the main synchronized state, which become a fuzzy cluster. With further increase of the control parameter, more oscillators separate, resulting in the appearance of the chimera states and, finally, the rotating wave. We find the wide region in the parameter space in which the so-called imperfect chimera state appears. The imperfect chimera state is characterized by a certain, small number of oscillators (solitary states [26]), which escape from the synchronized chimeras cluster (type I imperfect chimeras) or behave differently than most of the uncorrelated pendula (type II imperfect chimeras). The occurrence of the type II imperfect chimera states has been observed both in numerical and experimental studies in [25] (for a different model, i.e, a system of coupled metronomes). Here we give evidence of the existence of type I imperfect chimeras and uncover the mechanisms of the occurrence of imperfect chimera states and follow the transitions between them. We show that in a type I imperfect chimera state, the escaped elements oscillate with different average frequencies than the rest of the nodes.

II. MODEL

Since nonlocality of the coupling is the most important ingredient for chimera states, we consider a ring of N nonlocally coupled pendulumlike nodes. Coupling is introduced in such a way that each pendulum is connected to its P nearest neighbors to the left and to the right with equal strength. The phase of each pendulum is described as follows:

$$m\ddot{\theta}_i + \varepsilon\dot{\theta}_i = \frac{\mu}{2P+1}\sum_{j=i-P}^{i+P}\sin(\theta_j - \theta_i - \alpha), \qquad (1)$$

where $i = 1,\ldots,N$, α is a phase lag, ε is a damping coefficient, m is the mass of a single pendulum, and μ is a coupling coefficient. Equation (1) may be interpreted as the extension of the Kuramoto model to the second-order differential equations (i.e., Kuramoto model with inertia) [27,28].

We fix the default parameter values $m = 1.0$, $\varepsilon = 0.1$ and coupling radius $r = 0.4$ (i.e., $P = 40$, $N = 100$). The results of the numerical simulations are presented on frequency plots, where the momentary frequency ω is defined as mean phase velocities for each oscillator, i.e., $\omega_i(t) = \int_0^T \dot{\theta}_i(t+\tau)d\tau/T$ (we consider $T = 200$ because this is an adequate value to detect short time period imperfectness in imperfect chimera states).

If the system (1) is synchronized, then it can be reduced to the second-order linear differential equation: $m\ddot{\theta} + \varepsilon\dot{\theta} = -\mu\sin(\alpha)$. Synchronized elements tend to rotations described by $\theta(t) = -\frac{1}{\varepsilon^2}\{m\exp(-\frac{\varepsilon}{m}t)[v_0\varepsilon + \mu\sin(\alpha)] - (\theta_0\varepsilon + mv_0)\varepsilon + \mu\sin(\alpha)(t\varepsilon - m)\}$, where θ_0, v_0 are the initial values of position and velocity.

The master stability approach [29] allows one to show that the state of the complete synchronization is stable for $\alpha < \pi/2$.

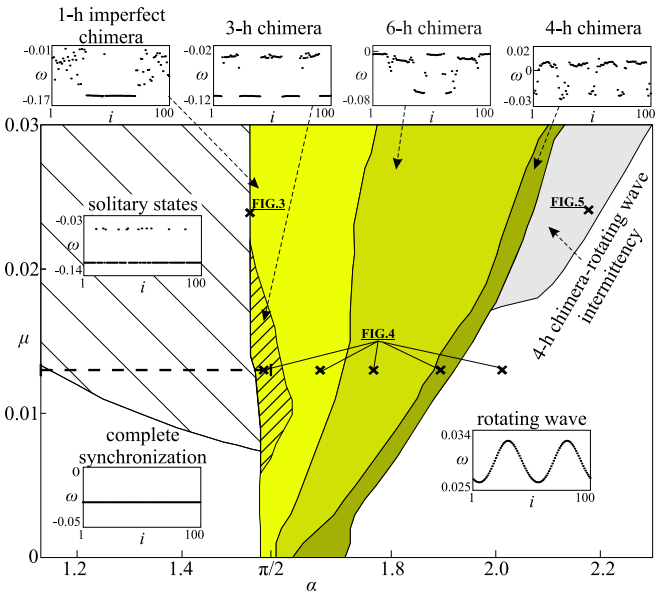

FIG. 1. (Color online) Dependence of possible spatiotemporal patterns on parameters α and μ. The crosses and dashed line denote parameter values (α, μ) for which the behavior of the system (1) is illustrated. Insets: Snapshots of typical states.

III. NUMERICAL SIMULATIONS AND DISCUSSIONS

System (1) is multistable, which means that there exist several attractors for a given set of parameters. Multistability is a common behavior in the coupled systems. Trying to understand the evolution scenario of solutions in the system, we continued just one solution throughout the parameter plane denoted as (α, μ) (the endpoint of the trajectory at old parameter values is used as the starting point for the new values of parameters).

The diversity of the obtained behaviors, including the complete synchronization, the solitary state, the imperfect one-headed chimera states, six- and four-headed clustered chimera, the rotating waves, and the intermittency between four-headed clustered chimera and the rotating wave, is presented in Fig. 1.

In the numerical simulations, we calculated the trajectory of a solitary state for $\mu = 0.015$ and $\alpha = 1.5$, then we continued this solution for increasing μ (until $\mu = 0.03$) and decreasing μ (until $\mu = 0.007$, reaching the complete synchronization region). In this way, we have obtained the set of trajectories and, for each one, we have set their endpoints as the starting points and have continued the solutions with decreasing and increasing α (for which we have obtained the transition from solitary state through chimeras to the rotating wave). Having the set of endpoints of trajectories calculated for $\mu = 0.007$ and $\alpha \in [1.1,2.3]$, we continued these solutions with decreasing μ, until $\mu = 0$. The step size for parameter μ is equal to 0.001 and the step size of α is equal to 0.01. The reason why we preferred to obtain the lower part of the diagram with decreasing μ is for the region of complete synchronization, from which much longer calculations should be performed or small perturbations should be added to obtain its destabilization with increasing α for $\alpha > \pi/2$.

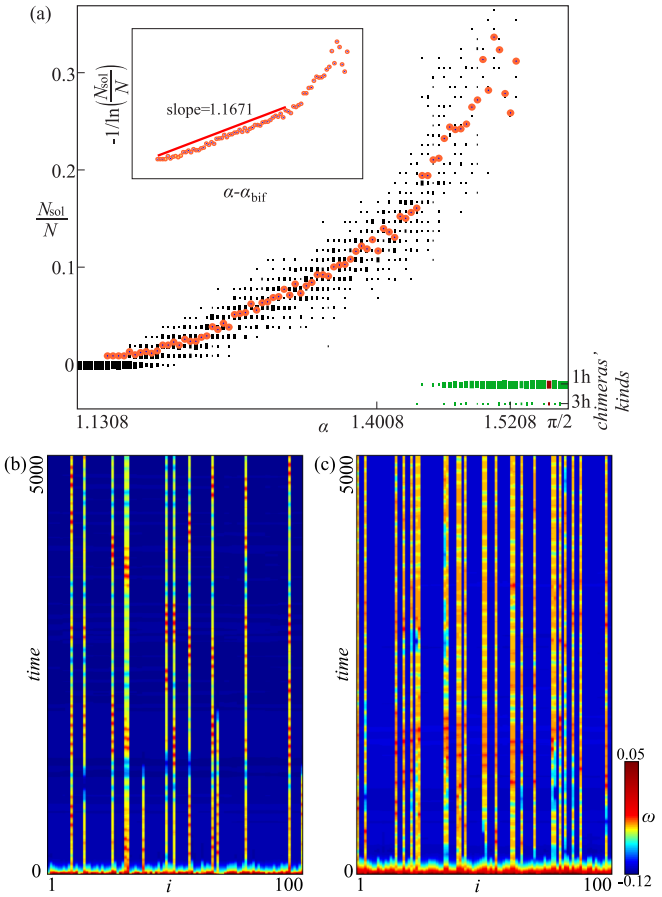

FIG. 2. (Color online) (a) The ratio of the number of solitary states $N_{\rm sol}$ to all elements N and kinds of occurring chimeras depending on parameter α. The size of the boxes indicates the probability of the occurrence of a certain state obtained for 20 randomizations (the smaller the box, the less probable the state). Orange (gray) dots stand for the mean value of $N_{\rm sol}/N$. The coupling coefficient is fixed at $\mu = 0.013$ (dashed line in Fig. 1). Inset: The $-1/\ln(N_{\rm sol}/N)$ vs $(\alpha - \alpha_{\rm bif})$ ($\alpha_{\rm bif} = 1.156$ value for each first solitary state that occurs) is presented. The number of solitary oscillators decreases exponentially, $N_{\rm sol} \sim \exp(-1/\alpha)$, as $\alpha \to \alpha_{\rm bif}$; (b),(c) time plots of frequencies for (b) $\alpha = 1.4008$ and (c) $\alpha = 1.5208$ (11 and 27 solitary states, respectively).

In a certain domain in parameter space (α, μ) (white dashed region in Fig. 1), we observe the solitary state region where one or a few oscillators escaped from the main, synchronized state. We call these split elements the solitary states. Due to the fact of such separation, the main cluster is fuzzy. Such dynamics of the system represents the phenomenon of spatial chaos, i.e., sensitive dependence on the space coordinates.

The number of solitary states appearing from random initial conditions is strongly related to the distance of the chosen parameters to the boundaries of the solitary state region indicated in Fig. 1. We may observe that the closer to the complete synchronization region, the less solitary states occur, and the closer to the imperfect chimera region, the more solitary states emerge. This phenomenon is presented in Fig. 2(a) for varied parameter α and the fixed coupling parameter. The ratio of the average number of the escaped oscillators to the number

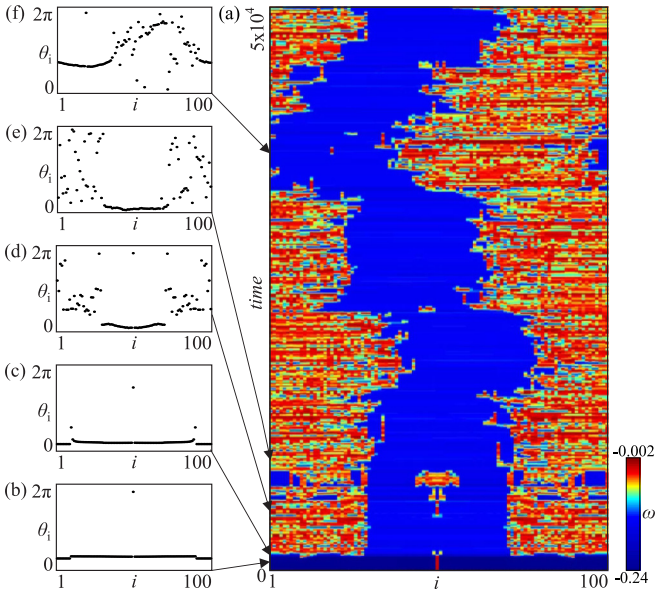

FIG. 3. (Color online) Creation and dynamics of imperfect chimera (solitary state is set as initial condition) presented in (a) time plot of frequencies ω for $\mu = 0.024$ and $\alpha = 1.5308$, (b)–(f) snapshots of phases.

of all elements obeys exponential law [inset in Fig. 2(a)]. The slope equals 1.1671 and the intercept equals 0.1963, hence the ratio N_{sol}/N depends on α in the following manner: $N_{\mathrm{sol}}/N = \exp[1/(-1.1671\alpha - 0.1963)]$.

Typical examples of solitary state patterns obtained for random initial conditions are shown in Figs. 2(b) and 2(c). Note that with the increase of α, the number of solitary states increase, and that in the time evolution, some solitary states can lose stability and return to the synchronized cluster, as seen in Fig. 2(b).

As the synchronous state is stable for $\alpha < \pi/2$, this means that for a lag parameter slightly smaller than $\pi/2$, we observe the following multistability: the coexistence of complete synchronization, the solitary states, and one-headed and three-headed chimera states.

For α close to $\pi/2$, we observe the creation of the special type of chimera states which we call imperfect chimera states. An imperfect chimera state is defined as the state with a certain number of oscillators split from the synchronized domain. The escaped elements oscillate with different average frequencies (Poincaré rotation number). The occurrence of such elements is in sharp contrast to the classical, perfect chimera state.

The mechanism for the creation of chimera states found in system (1) is characterized by the appearance of solitary states. By increasing control parameter α in the solitary state region, more and more oscillators leave the synchronous group, which results in the appearance of the chimera state. The other possible scenario is also the separation of successive elements, but along with time, which is presented in the frequency time plot and the snapshots of the phase during the formation of the chimera state in Figs. 3(a)–3(e). First one element splits the synchronized cluster, as shown in Fig. 3(b). Next, two more elements split [Fig. 3(c)] and, immediately after it, the chimera state is created. Note that the created chimera is imperfect, since two nodes are split from the synchronized cluster [Fig. 3(a)]. After a certain time, the elements, which make the chimera imperfect, stick to the main cluster in order to form a perfect chimera state. As may be seen, the created chimera is perfect only for a certain time, and then an imperfectness appears again—one element escapes from the newly formed synchronized cluster [Fig. 3(d)]. The coherent group moves with significantly higher negative frequency than the incoherent region, where the pendula constantly make extra oscillations. Pendula in the coherent cluster rotate, while those in the incoherent region perform the motion, which is the combination of rotations and oscillations. The same combined motion is performed by split elements. As we have started from the symmetric initial condition, the obtained chimera is symmetric, but due to asymmetry of numerical methods after a certain time, the symmetry is broken [Fig. 3(e)].

For some parameter values, the obtained one-headed chimera is perfect for the long time, which turns out to be transient because for even longer calculations imperfectness is always achieved.

In Figs. 4(a) and 4(b), we observe one-headed imperfect and three-headed chimera states coexisting for the same parameters. Figure 4(c) displays that with the increase of lag parameter α, the number of the separated oscillators in the imperfect chimera grows. The escaped nodes are not just solitary elements here, but they create whole islands split from the synchronous state. The emerged islands always occur in the middle of the emerging coherent cluster because with further increase of α, this island becomes the cluster in the six-headed chimera [Fig. 4(d)]. Other clusters are three coherent domains formed from the incoherent domain of the one-headed imperfect chimera. Thus, the six-headed chimera consist of four coherent clusters with lower negative frequency, whose motion is a combination of rotation and oscillation, and two coherent clusters with higher negative frequency, which are created from the coherent cluster of the one-headed chimera state. The six-headed clustered chimera state is often disturbed with imperfect one-headed chimera (this disturbance is less common for $\mu < 0.15$). Also with the increase of α, the six-headed chimera is disturbed by the incoherent motion.

With further increase of the lag parameter, we obtain regular motion, which is a four-headed clustered chimera [Fig. 4(e)]. The obtained four-headed clustered chimera is created from the six-headed chimera by transformation of coherent regions with the biggest negative frequency from the six-headed chimera to incoherent ones. The coherent clusters both rotate and oscillate here. With increasing α, incoherent regions disappear and a rotating wave with a positive frequency value [Fig. 4(f)] appears.

As can be seen in the snapshots in Fig. 1, for one-headed and three-headed chimera, the incoherent elements move more slowly than the coherent ones. For the six-headed chimera, the frequency of incoherent elements is between the lower and upper chimera clusters. For the four-headed chimera, the synchronized clusters start moving in another direction (the frequency becomes positive), but regarding the absolute value of the frequency, the incoherent elements move faster (but in another direction).

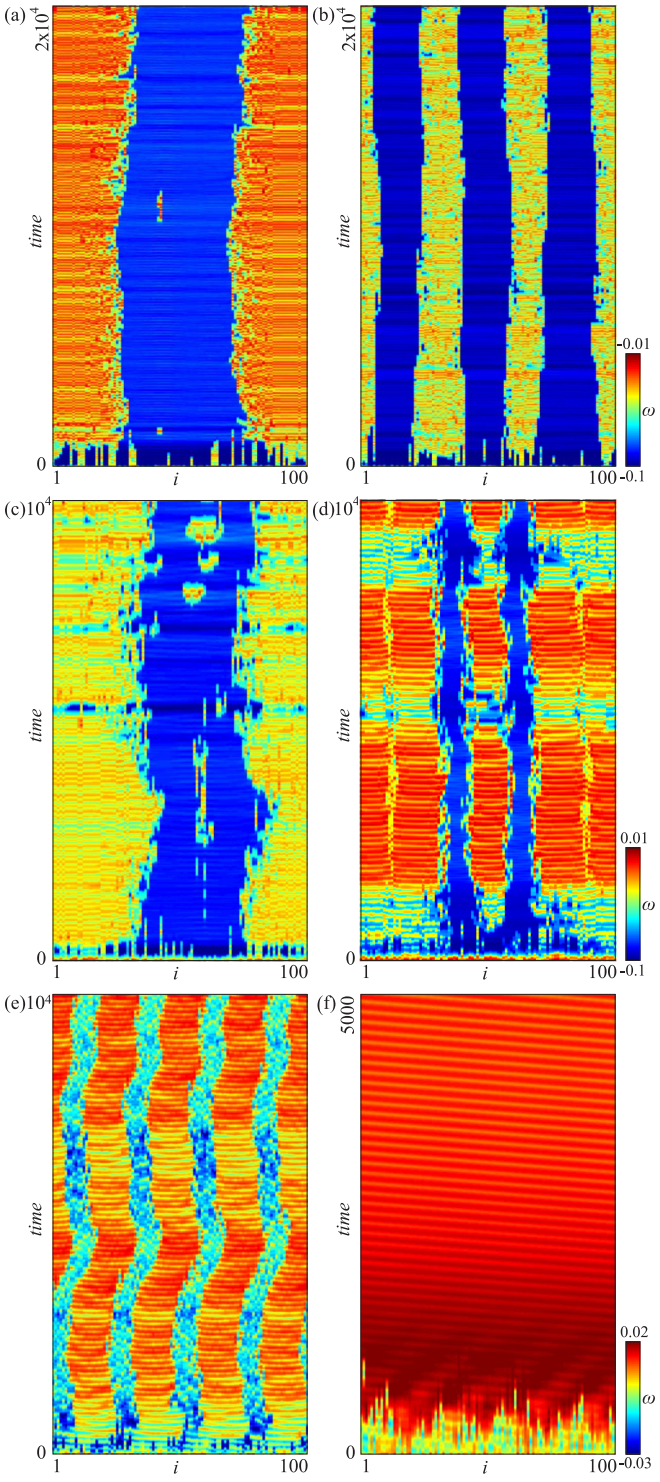

FIG. 4. (Color online) Frequency time plots for (a),(b) coexisting one- and three-headed chimera states for $\alpha = 1.5558$ [value indicated by red (dark gray) boxes in Fig. 2], (c) the growth of the number of split elements and the creation of islands for imperfect one-headed chimera with the increase of α ($\alpha = 1.6708$), (d) six-headed clustered chimera state ($\alpha = 1.7708$), (e) four-headed clustered chimera state ($\alpha = 1.9008$), and (f) rotating wave ($\alpha = 2.0208$). All plots are obtained for $\mu = 0.013$ and random initial conditions.

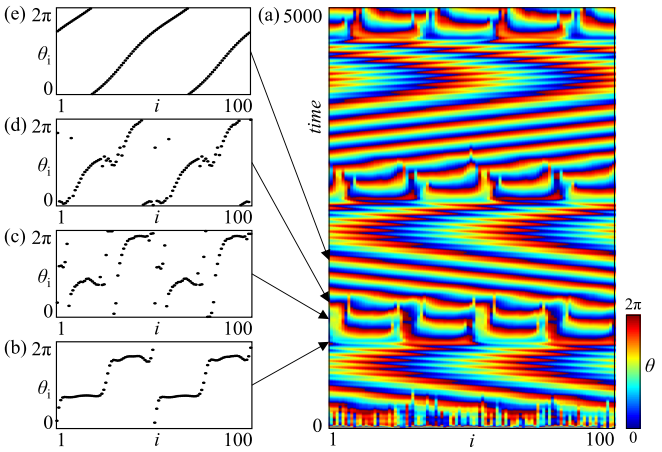

FIG. 5. (Color online) (a) Space-time plot of the phase for the rotating wave "interweaving" with the four-headed clustered chimera (random initial conditions, $\mu = 0.024$ and $\alpha = 2.1908$); (b)–(e) phase snapshots with the increase of time.

In the region of intermittency between the four-headed clustered chimera and the rotating wave, the following scenario is looped [Fig. 5(a)]. At the beginning, the rotating wave [Fig. 5(b)] falls apart and becomes a four-headed clustered chimera. The obtained chimera has four heads, which create two shifted clusters [Fig. 5(c)]. The same coherent clusters are nearly in-phase, while between successive coherent clusters they are in the antiphase. After a while, we may observe the creation of the rotating wave. The snapshot shows that the incoherent domains in the four-headed clustered chimera [Fig. 5(d)] slowly subject to the synchronized parts. Finally, they stick to the coherent domain and create the rotating wave [Fig. 5(e)].

IV. CONCLUSIONS

We have identified a different type of spatiotemporal pattern, i.e., imperfect chimera states, in the Kuramoto model with inertia. This type of behavior is observed in a wide range of coupling parameters and is characterized by a certain number of oscillators that have escaped from the synchronized chimera's cluster. The escaped elements typically oscillate with different average frequencies. We identify a mechanism for the creation of chimera states via the appearance of the solitary states. This transition is initiated by the escape of one or a few oscillators from the main synchronized state, which becomes a fuzzy cluster. With further increase of the control parameter, more oscillators separate, resulting in the appearance of different types of a chimera state and, finally, lead to the creation of the rotating wave. This indicates a common, possibly universal transition between coherent and incoherent states in the networks of very different nature.

Our numerical experiments confirm that imperfect chimeras are characteristic objects in the systems with inertia. Here, we have obtained them for a Kuramoto model with inertia; previously, [25], we have reported such chimeras, both in simulations and experiments, for a ring of coupled self-excited pendula (metronomes or Huygens clocks). In such systems, the complete synchronization is achieved due to the energy transfer between oscillators [30]. At the chimera state, one

observes the permanent energy transfer between the coupled oscillators (there is no energy transfer only in the state of complete synchronization). This transfer perturbs the behavior of the oscillators close to the boundary between the coherent and incoherent oscillators, leading apparently to imperfection; see, e.g., Figs. 3 and 4(c), where the imperfect chimeras are obtained close to these boundaries. The mechanism for the imperfect chimera states can also be connected to the appearance of the driven intrinsic localized mode in the network of coupled oscillators [31], but to verify this hypothesis further studies are necessary.

ACKNOWLEDGMENT

This work has been supported by the Polish National Science Centre, MAESTRO Programme - Project No. 2013/08/A/ST8/00/780.

[1] Y. Kuramoto and D. Battogtokh, Nonlinear Phenom. Complex Syst. **5**, 380 (2002).
[2] D. M. Abrams and S. H. Strogatz, Phys. Rev. Lett. **93**, 174102 (2004).
[3] D. M. Abrams, R. Mirollo, S. H. Strogatz, and D. A. Wiley, Phys. Rev. Lett. **101**, 084103 (2008).
[4] O. E. Omelchenko, Y. L. Maistrenko, and P. A. Tass, Phys. Rev. Lett. **100**, 044105 (2008).
[5] C. R. Laing, Physica D **238**, 1569 (2009).
[6] C. R. Laing, Phys. Rev. E **81**, 066221 (2010).
[7] E. A. Martens, Phys. Rev. E **82**, 016216 (2010).
[8] E. A. Martens, C. R. Laing, and S. H. Strogatz, Phys. Rev. Lett. **104**, 044101 (2010).
[9] O. E. Omelchenko, M. Wolfrum, and Y. L. Maistrenko, Phys. Rev. E **81**, 065201(R) (2010).
[10] I. Omelchenko, Y. L. Maistrenko, P. Hövel, and E. Schöll, Phys. Rev. Lett. **106**, 234102 (2011).
[11] M. Wolfrum and O. E. Omel'chenko, Phys. Rev. E **84**, 015201 (2011).
[12] M. Wolfrum, O. E. Omelchenko, S. Yanchuk, and Y. L. Maistrenko, Chaos **21**, 013112 (2011).
[13] O. E. Omelchenko, M. Wolfrum, S. Yanchuk, Y. L. Maistrenko, and O. Sudakov, Phys. Rev. E **85**, 036210 (2012).
[14] M. R. Tinsley, S. Nkomo, and K. Showalter, Nat. Phys. **8**, 662 (2012); S. Nkomo, M. R. Tinsley, and K. Showalter, Phys. Rev. Lett. **110**, 244102 (2013).
[15] J. Hizanidis, V. Kanas, A. Bezerianos, and T. Bountis, Int. J. Bifurc. Chaos **24**, 1450030 (2014).
[16] A. Yeldesbay, A. Pikovsky, and M. Rosenblum, Phys. Rev. Lett. **112**, 144103 (2014).
[17] G. C. Sethia and A. Sen, Phys. Rev. Lett. **112**, 144101 (2014).
[18] A. Zakharova, M. Kapeller, and E. Schöll, Phys. Rev. Lett. **112**, 154101 (2014).
[19] M. J. Panaggio and D. M. Abrams, arXiv:1403.6204.
[20] Y. L. Maistrenko, A. Vasylenko, O. Sudakov, R. Levchenko, and V. L. Maistrenko, Int. J. Bifurc. Chaos **24**, 1440014 (2014).
[21] A. M. Hagerstrom, T. E. Murphy, R. Roy, P. Hövel, I. Omelchenko, and E. Schöll, Nat. Phys. **8**, 658 (2012).
[22] L. Larger, B. Penkovsky, and Yu. Maistrenko, arXiv:1411.4483.
[23] L. Larger, B. Penkovsky, and Y. L. Maistrenko, Phys. Rev. Lett. **111**, 054103 (2013).
[24] E. A. Martens, S. Thutupalli, A. Fourriere, and O. Hallatschek, Proc. Natl. Acad. Sci. **110**, 10563 (2013).
[25] T. Kapitaniak, P. Kuzma, J. Wojewoda, K. Czolczynski, and Yu. Maistrenko, Sci. Rep. **4**, 6379 (2014).
[26] Yu. Maistrenko, B. Penkovsky, and M. Rosenblum, Phys. Rev. E **89**, 060901(R) (2014).
[27] S. Olmi, A. Navas, S. Boccaletti, and A. Torcini, Phys. Rev. E **90**, 042905 (2014).
[28] T. Bountis, V. G. Kanas, J. Hizanidis, and A. Bezerianos, Europhys. J. Spec. Top. **223**, 721 (2014).
[29] L. M. Pecora and T. L. Carroll, Phys. Rev. Lett. **80**, 2109 (1998).
[30] M. Kapitaniak, K. Czolczynski, P. Perlikowski, A. Stefanski, and T. Kapitaniak, Phys. Rep. **517**, 1 (2012).
[31] R. Basu Thakur, L. Q. English, and A. J. Sievers, J. Phys. D: Appl. Phys. **41**, 015503 (2008).